

A NUMERICAL METHOD FOR SOLVING THE GENERALIZED TANGENT VECTOR OF HYPERBOLIC SYSTEMS *

MICHAEL HERTY [†] AND YIZHOU ZHOU [‡]

Abstract. This work is concerned with the computation of the first-order variation for one-dimensional hyperbolic partial differential equations. In the case of shock waves the main challenge is addressed by developing a numerical method to compute the evolution of the generalized tangent vector introduced by Bressan and Marson (1995) [5]. Our basic strategy is to combine the conservative numerical schemes and a novel expression of the interface conditions for the tangent vectors along the discontinuity. Based on this, we propose a simple numerical method to compute the tangent vectors for general hyperbolic systems. Numerical results are presented for Burgers' equation and a 2×2 hyperbolic system with two genuinely nonlinear fields.

Key words. Conservative schemes, Generalized tangent vectors, Interface conditions

MSC codes. 35L65, 49K40, 65M08

1. Introduction. This paper deals with the computation of the first-order variation for the system of conservation laws in one dimension:

$$(1.1) \quad u_t + f(u)_x = 0, \quad x \in \mathbb{R},$$

$$(1.2) \quad u|_{t=0} = \bar{u}(x).$$

Here $u \in \mathbb{R}^n$ is the unknown and $f : \mathbb{R}^n \rightarrow \mathbb{R}^n$ is a smooth function of u . We assume that the system (1.1) is strictly hyperbolic, and that each characteristic field is either linearly degenerate or genuinely nonlinear in the sense of Lax [22].

It has been shown that the evolution operator $\mathcal{S}_t : \bar{u}(\cdot) \rightarrow u(t, \cdot) = \mathcal{S}_t \bar{u}(\cdot)$ generated by the conservation law (1.1) is generically non-differentiable in $L^1(\mathbb{R})$, see e.g. [5, 17] for examples. Therefore, the concept of generalized tangent vector (GTV) has been proposed [5] for piecewise Lipschitz continuous solution $u(t, \cdot)$ with a finite number of N discontinuities. The differential is described by measures with an absolutely continuous part $v(t, \cdot) \in L^1(\mathbb{R})$ and a singular part. The latter is determined as a variation of the shift $\xi_\alpha(t)$ at each jump location $x_\alpha(t)$ ($\alpha = 1, 2, \dots, N$). It has been shown ([5]) that ξ_α satisfies an ordinary differential equation and v solves the linear equation

$$(1.3) \quad v_t + A(u)v_x + [DA(u)v]u_x = 0,$$

*

Funding: The first author is funded by the Deutsche Forschungsgemeinschaft (DFG, German Research Foundation) - SPP 2410 Hyperbolic Balance Laws in Fluid Mechanics: Complexity, Scales, Randomness (CoScaRa) within the Project(s) HE5386/26-1 (Numerische Verfahren für gekoppelte Mehrskalenprobleme, 525842915), (Zufällige kompressible Euler Gleichungen: Numerik und ihre Analysis, 525853336) HE5386/27-1, and under HE5386/25-1 Differenzierbare Programmierung für Strömungen mit Diskontinuitäten (513718742). Furthermore, support received funding from the European Union's Horizon Europe research and innovation programme under the Marie Skłodowska-Curie Doctoral Network Datahyking (Grant No.101072546) is acknowledged. The second author is funded by Alexander von Humboldt Foundation (Humboldt Research Fellowship Programme for Postdocs).

[†]Chair in Numerical Analysis, IGPM, RWTH Aachen University, Templergraben, 55, D-52062 Aachen, Germany (herty@igpm.rwth-aachen.de)

[‡]Corresponding author, IGPM, RWTH Aachen University, Templergraben, 55, D-52062 Aachen, Germany (zhou@igpm.rwth-aachen.de)

outside the points $x_\alpha(t)$ where $u(t, \cdot)$ suffers a discontinuity. Along each line $x = x_\alpha(t)$, v satisfies the interface conditions for $t > 0$

$$(1.4) \quad \Psi_\alpha(v^-, v^+; u^-, u^+, \xi_\alpha) = 0, \quad \alpha = 1, 2, \dots, N.$$

Here, $v^+ = \lim_{x \rightarrow x_\alpha^+} v(t, x)$ and $v^- = \lim_{x \rightarrow x_\alpha^-} v(t, x)$ represent the left and right limits of v at the point of discontinuity $x = x_\alpha(t)$. Note that the interface conditions depend on ξ_α as well as the limits u^- and u^+ . We refer to Section 2 for the explicit formula (2.4).

At this point, we briefly review other theoretical results treating differentiability and related questions of hyperbolic conservation laws. In [3], the Lipschitz continuous dependence of \mathcal{S}_t in L^1 on the initial data has been established. Furthermore, an adjoint calculus and optimality conditions are derived in [6]. In the scalar 1D case, results on differentiability have been extended from directional to Fréchet-type differentiability [30, 7, 31, 32, 29] in the case of piecewise C^1 initial data. Moreover, a sensitivity and adjoint calculus is developed for both initial and initial-boundary value problems. An alternative variational calculus, referred to as shift-differentiability based on horizontal shifts of the graph, is developed in [4] for the scalar case and in [2] for the system's case. We refer to the references therein for further details.

The main goal of the present work is to propose a (simple) numerical method for the computation of the generalized tangent vector (v, ξ_α) introduced in [5]. In particular, our main concern is to develop a strategy dealing with interface conditions (1.4) for the GTV. Our work is motivated by numerical methods for hyperbolic conservation laws. Therein, computing discontinuous solutions of (1.1), can be obtained using conservative schemes that preserve the Rankine–Hugoniot condition

$$s[u] = [f(u)] \quad \text{at the jump position } x = x_\alpha(t).$$

Here $s = x'_\alpha(t)$ is the shock speed and $[u] = u^+ - u_-$. This strategy can also be used to compute the generalized tangent vector. The interface conditions (1.4) can be regarded as the formal differentiation of the Rankine–Hugoniot condition in the case of a single discontinuity of a single family, see [8, 17]. Namely,

$$\dot{s}[u] + s[\dot{u}] = [\dot{f}] = [A(u)\dot{u}].$$

Here the dot means the formal differentiation with respect to the initial data. Motivated by Lemma 2.1 in [5], we write $\dot{s} = \xi'_\alpha$ and $\dot{u} = w = v + \xi_\alpha u_x$ to conclude

$$(1.5) \quad \xi'_\alpha[u] + s[w] = [A(u)w].$$

In the present paper, we rigorously verify the above formal derivation in the framework of [5] and present a method for their numerical computation. To illustrate the method, we first deal with a simple case of only a single jump discontinuity in the original problem (1.1)-(1.2). In this case, we use the formula (1.5) within conservative schemes. The interface conditions (1.4) are shown to be preserved without additional numerical treatment. For the case of multiple discontinuities, we assume, that there is no interaction between two discontinuities. Finally, we present a simple way to combine the results for different jumps and obtain the generalized tangent vector on the whole domain.

Numerical methods for discretizing the sensitivity equation in hyperbolic conservation laws have been an active research topic. These methods are particularly

relevant to numerical computations in optimal control problems for hyperbolic conservation laws. In [8, 11, 15, 16], the authors develop a numerical method to compute the sensitivity equation by adding delta-type source terms. We remark that our method is similar to this series of work in computing Riemann problems. However, our method is based on the rigorous theoretical result of the GTV in [5]. Unlike these works, our numerical strategy for the GTV does not need piecewise constant assumption and can be extended to any conservative schemes. More detailed comparisons can be found in Remark 4.2. In [17], the authors develop an algorithmic differentiation framework for computing the sensitivity equation. In the works [12, 13], the convergence of a modified Lax-Friedrichs scheme for the sensitivity equation has been demonstrated even in the presence of shocks. Additionally, convergence results for state schemes that satisfy a discrete one-sided Lipschitz condition, along with their corresponding adjoint schemes, are presented in [30, 27, 28], while implicit-explicit methods are discussed in [1, 20]. In [20], a relaxation approximation is exploited in the tangent vector calculus, and corresponding schemes are derived. Further examples include finite volume, Lagrangian methods, and vanishing viscosity approach in [19, 18, 9, 25]. We would like to stress the fact that the sensitivity analysis of hyperbolic problems has a rich field of application in engineering [14, 24, 26, 10, 21].

The paper is organized as follows. In Section 2, we review the theoretical results of the generalized tangent vector. Section 3 is devoted to deduction of interface conditions and two illustrative examples are presented. In Section 4, we give a numerical method for computing the generalized tangent vector, and more numerical experiments are shown in Section 5. In Appendix A, we give some details of the proof in Section 3.

2. Preliminaries. This section briefly recalls the theoretical results of the generalized tangent vector (GTV) developed in [5].

First, we introduce some basic notations. For the flux term in (1.1), denote the Jacobian matrix $A(u) := f_u(u)$. By the strictly hyperbolic assumption, it has n real distinct eigenvalues $\lambda_1(u) < \lambda_2(u) < \dots < \lambda_n(u)$. For any two vectors $u, v \in \mathbb{R}^n$, we define the matrix

$$(2.1) \quad \bar{A}(u, v) = \int_0^1 A(\theta u + (1 - \theta)v) d\theta.$$

For $i = 1, \dots, n$, the i -th eigenvalue, left eigenvector and right eigenvector of $\bar{A}(u, v)$ will be denoted by $\lambda_i(u, v)$, $l_i(u, v)$ and $r_i(u, v)$ respectively. We assume that the ranges of the eigenvalues $\lambda_i(u, v)$ do not overlap for any (u, v) . Because of the regularity of A and the strict hyperbolic assumption, $\lambda_i(u, v)$, $l_i(u, v)$ and $r_i(u, v)$ are all C^1 functions.

As in [5], we only consider the piecewise Lipschitz continuous solution $u(t, x)$ with N discontinuities. For each $\alpha = 1, \dots, N$, let $x_\alpha(t)$ be the position of the α -th discontinuity of $u(t, x)$ at time t . Assume that the discontinuity at $x = x_\alpha(t)$ corresponds to the k_α -th characteristic family, the Rankine-Hugoniot and the entropy admissibility conditions imply

$$\begin{aligned} x'_\alpha(t) &= \lambda_{k_\alpha}(u^+, u^-), \\ \langle l_i(u^+, u^-), u^+ - u^- \rangle &= 0, \quad \forall i \neq k_\alpha, \\ \lambda_{k_\alpha}(u^+, u^+) &\leq \lambda_{k_\alpha}(u^+, u^-) \leq \lambda_{k_\alpha}(u^-, u^-). \end{aligned}$$

Here $u^+ = \lim_{x \rightarrow x_\alpha^+} u(t, x)$ and $u^- = \lim_{x \rightarrow x_\alpha^-} u(t, x)$ represent the left and right limits of u at the discontinuity $x = x_\alpha(t)$.

In studying the first-order variation of (1.1), some regularity conditions for the perturbed solution u^ϵ should be given. Namely,

DEFINITION 2.1. *Let $u = u(x)$ be a piecewise Lipschitz continuous function on \mathbb{R} with N simple discontinuities. A path γ is a Regular Variation (R.V.) for u if, for $\epsilon \in [0, \epsilon_0]$, all functions $u^\epsilon = \gamma(\epsilon)$ are piecewise Lipschitz continuous, with jumps at points $x_1^\epsilon < \dots < x_N^\epsilon$ depending continuously on ϵ . Moreover, the Lipschitz constant of u is independent of ϵ .*

With these preparations, the main result in [5] can be stated:

THEOREM 2.2. *Let $u = u(t, x)$ be a piecewise Lipschitz continuous solution of (1.1) with N simple discontinuities. Let $(\bar{v}, \bar{\xi}) \in L^1(\mathbb{R}) \times \mathbb{R}^N$ be a tangent vector to the initial data $u(0, x) = \bar{u}(x)$, generated by the R.V. $\epsilon \mapsto \bar{u}^\epsilon$, and call $u^\epsilon = u^\epsilon(t, x)$ the solution of (1.1) with initial condition \bar{u}^ϵ . Then there exists $\tau_0 > 0$ such that, for all $t \in [0, \tau_0]$, the path $\epsilon \mapsto u^\epsilon(t, \cdot)$ is a R.V. for $u(t, \cdot)$, generating the tangent vector $(v(t), \xi(t))$. The vector $(v(t), \xi(t))$ is the unique solution of the problem:*

$$(2.2) \quad v_t + A(u)v_x + [DA(u)v]u_x = 0, \quad v(0, x) = \bar{v}(x)$$

outside the discontinuities of u , while, for $\alpha = 1, \dots, N$,

$$(2.3) \quad \xi'_\alpha = D\lambda_{k_\alpha}(u^+, u^-) \cdot (v^+ + \xi_\alpha u_x^+, v^- + \xi_\alpha u_x^-), \quad \xi_\alpha(0) = \bar{\xi}_\alpha,$$

$$(2.4) \quad \begin{aligned} & \langle Dl_i(u^+, u^-) \cdot (v^+ + \xi_\alpha u_x^+, v^- + \xi_\alpha u_x^-), u^+ - u^- \rangle \\ & + \langle l_i(u^+, u^-), (v^+ + \xi_\alpha u_x^+ - v^- - \xi_\alpha u_x^-) \rangle = 0, \quad \forall i \neq k_\alpha \end{aligned}$$

along each line $x = x_\alpha(t)$ where $u(t, \cdot)$ suffers a discontinuity, in the k_α -th characteristic direction.

This theorem provides the evolution equations for $v = v(t, x)$ and $\xi = \xi(t)$. Note that the formula (2.4) is just the aforementioned interface condition (1.4). The first-order variation u_ϵ can be computed from

$$(2.5) \quad u_\epsilon = u + \epsilon v + \sum_{\xi_\alpha < 0} (u(x_\alpha^+) - u(x_\alpha^-)) \chi_{[x_\alpha + \epsilon \xi_\alpha, x_\alpha]} - \sum_{\xi_\alpha > 0} (u(x_\alpha^+) - u(x_\alpha^-)) \chi_{[x_\alpha, x_\alpha + \epsilon \xi_\alpha]}.$$

Here $u(x_\alpha^\pm) = \lim_{x \rightarrow x_\alpha^\pm} u(t, x)$ and $\chi_{[a, b]} = \chi_{[a, b]}(x)$ is the characteristic function of the interval $[a, b]$. The construction of u^ϵ can be understood in the following way: starting with u , adding ϵv and then shifting by $\epsilon \xi_\alpha$ each point x_α where u has a jump.

3. Interface conditions for the GTV. We aim to present a numerical method for solving (2.2)-(2.4). Recall that the equation (2.2) is only valid outside the shock position $x = x_\alpha(t)$, i.e., $(t, x) \neq (t, x_\alpha(t))$. Along the discontinuity $x = x_\alpha(t)$, the ordinary differential equation (2.3)

$$\xi'_\alpha = D\lambda_{k_\alpha}(u^+, u^-) \cdot (v^+ + \xi_\alpha u_x^+, v^- + \xi_\alpha u_x^-)$$

and the interface conditions (2.4)

$$\begin{aligned} & \langle Dl_i(u^+, u^-) \cdot (v^+ + \xi_\alpha u_x^+, v^- + \xi_\alpha u_x^-), u^+ - u^- \rangle \\ & + \langle l_i(u^+, u^-), (v^+ + \xi_\alpha u_x^+ - v^- - \xi_\alpha u_x^-) \rangle = 0, \quad \forall i \neq k_\alpha \end{aligned}$$

hold true. Next, we will present new expressions for (2.3) and (2.4), that allows for a simple numerical treatment in Section 4.

Recall the proof in [5] where the variables

$$(3.1) \quad w_\alpha = v + \xi_\alpha u_x, \quad y = x - x_\alpha(t)$$

are introduced to analyze the α -th jump in a neighborhood of $x_\alpha(t)$. The equation for $w_\alpha = w_\alpha(y, t)$ reads

$$\partial_t w_\alpha + [A(u) - x'_\alpha I] \partial_y w_\alpha + DA(u)(\partial_y u) w_\alpha - \xi'_\alpha \partial_y u = 0.$$

Moreover, the relations (2.3) and (2.4) become

$$(3.2) \quad \xi'_\alpha(t) = D\lambda_{k_\alpha}(u^+, u^-)(w_\alpha^+, w_\alpha^-)$$

$$(3.3) \quad \langle l_i(u^+, u^-), w_\alpha^+ - w_\alpha^- \rangle + \langle Dl_i(u^+, u^-)(w_\alpha^+, w_\alpha^-), u^+ - u^- \rangle = 0, \quad i \neq k_\alpha.$$

Assume that the solution is sufficiently smooth except for the position $y = 0$. We can rewrite the equation to the conservative form

$$(3.4) \quad \partial_t w_\alpha + \partial_y [A(u)w_\alpha - x'_\alpha w_\alpha - \xi'_\alpha u] = 0.$$

Based on these preparations, we state

THEOREM 3.1. *The equation (3.2) is equivalent to the relation:*

$$(3.5) \quad \xi'_\alpha = \langle l_{k_\alpha}(u^+, u^-), [A(u^+) - \bar{A}(u^+, u^-)]w_\alpha^+ + [\bar{A}(u^+, u^-) - A(u^-)]w_\alpha^- \rangle.$$

Here $l_{k_\alpha}(u^+, u^-)$ is the left eigenvector of $\bar{A}(u^+, u^-)$ satisfying $\langle l_{k_\alpha}(u^+, u^-), u^+ - u^- \rangle = 1$. Moreover, the interface condition (3.3) is satisfied under the following relation:

$$(3.6) \quad x'_\alpha w_\alpha^+ - A(u^+)w_\alpha^+ + \xi'_\alpha u^+ = x'_\alpha w_\alpha^- - A(u^-)w_\alpha^- + \xi'_\alpha u^-,$$

which implies that the flux in (3.4) is continuous at $y = 0$.

In order to prove this theorem, we need the following Lemma.

LEMMA 3.2. *If $f \in C^2(G)$, the following relations hold for each $i = 1, 2, \dots, n$:*

$$\begin{aligned} \frac{\partial l_i}{\partial u^+}(\lambda_{k_\alpha} - \lambda_i)(u^+ - u^-) + l_i[A(u^+) - \bar{A}(u^+, u^-)] &= \frac{\partial \lambda_i}{\partial u^+} \langle l_i, u^+ - u^- \rangle, \\ \frac{\partial l_i}{\partial u^-}(\lambda_{k_\alpha} - \lambda_i)(u^+ - u^-) + l_i[\bar{A}(u^+, u^-) - A(u^-)] &= \frac{\partial \lambda_i}{\partial u^-} \langle l_i, u^+ - u^- \rangle. \end{aligned}$$

Here $\lambda_i = \lambda_i(u^+, u^-)$ is the i -th eigenvalue of $\bar{A}(u^+, u^-)$ and $l_i = l_i(u^+, u^-)$ is the corresponding (left) eigenvector.

We leave the proof of this lemma to Appendix A. We now prove Theorem 3.1 as follows.

Proof. Taking $i = k_\alpha$ in Lemma 3.2 and using $\langle l_{k_\alpha}, u^+ - u^- \rangle = 1$, we have

$$\frac{\partial \lambda_{k_\alpha}}{\partial u^+} = l_{k_\alpha}[A(u^+) - \bar{A}(u^+, u^-)], \quad \frac{\partial \lambda_{k_\alpha}}{\partial u^-} = l_{k_\alpha}[\bar{A}(u^+, u^-) - A(u^-)].$$

Then it follows that

$$\begin{aligned}\xi'_\alpha &= D\lambda_{k_\alpha}(u^+, u^-)(w_\alpha^+, w_\alpha^-) = \left\langle \frac{\partial \lambda_{k_\alpha}}{\partial u^+}, w_\alpha^+ \right\rangle + \left\langle \frac{\partial \lambda_{k_\alpha}}{\partial u^-}, w_\alpha^- \right\rangle \\ &= \langle l_{k_\alpha}[A(u^+) - \bar{A}(u^+, u^-)], w_\alpha^+ \rangle + \langle l_{k_\alpha}[\bar{A}(u^+, u^-) - A(u^-)], w_\alpha^- \rangle.\end{aligned}$$

This is the equation (3.5). Furthermore, we write (3.6) as

$$\xi'_\alpha(u^+ - u^-) = A(u^+)w_\alpha^+ - A(u^-)w_\alpha^- - x'_\alpha(w_\alpha^+ - w_\alpha^-).$$

Multiplying l_i on the left and using the fact $\langle l_i, u^+ - u^- \rangle = 0$ for any $i \neq k_\alpha$, we obtain

$$\begin{aligned}0 &= \langle l_i, A(u^+)w_\alpha^+ - A(u^-)w_\alpha^- - x'_\alpha(w_\alpha^+ - w_\alpha^-) \rangle, \\ &= \langle l_i, [A(u^+) - \bar{A}(u^+, u^-)]w_\alpha^+ + [\bar{A}(u^+, u^-) - A(u^-)]w_\alpha^- \rangle \\ &\quad + \langle l_i, \bar{A}(u^+, u^-)(w_\alpha^+ - w_\alpha^-) - x'_\alpha(w_\alpha^+ - w_\alpha^-) \rangle.\end{aligned}$$

Since $l_i \bar{A}(u^+, u^-) = \lambda_i l_i$ and $x'_\alpha = \lambda_{k_\alpha}$, we have

$$(3.7) \quad 0 = \langle l_i, [A(u^+) - \bar{A}(u^+, u^-)]w_\alpha^+ + [\bar{A}(u^+, u^-) - A(u^-)]w_\alpha^- \rangle + (\lambda_i - \lambda_{k_\alpha})\langle l_i, w_\alpha^+ - w_\alpha^- \rangle.$$

In order to simplify this equation, we take $i \neq k_\alpha$ in Lemma 3.2 and use the relation $\langle l_i, u^+ - u^- \rangle = 0$ to get

$$\begin{aligned}0 &= \frac{\partial l_i}{\partial u^+}(\lambda_{k_\alpha} - \lambda_i)(u^+ - u^-) + l_i[A(u^+) - \bar{A}(u^+, u^-)], \\ 0 &= \frac{\partial l_i}{\partial u^-}(\lambda_{k_\alpha} - \lambda_i)(u^+ - u^-) + l_i[\bar{A}(u^+, u^-) - A(u^-)].\end{aligned}$$

Substituting these into (3.7), we obtain

$$0 = \left\langle \frac{\partial l_i}{\partial u^+}(u^+ - u^-), w_\alpha^+ \right\rangle + \left\langle \frac{\partial l_i}{\partial u^-}(u^+ - u^-), w_\alpha^- \right\rangle + \langle l_i, w_\alpha^+ - w_\alpha^- \rangle.$$

This is the interface condition (3.3) and we complete the proof of Theorem 3.1. \square

Next, we illustrate Theorem 3.1 through two examples.

Example 1 (Burgers equation): The Riemann problem for the Burgers equation reads as

$$u_t + \left(\frac{u^2}{2} \right)_x = 0$$

with the initial data

$$u(x, 0) = \begin{cases} u^-, & x < 0, \\ u^+, & x \geq 0. \end{cases}$$

Here u^- and u^+ are two constants. Since there is only one shock, we drop the subscription α and write the generalized tangent vector in (3.2) and (3.4) as (ξ, w) . By a direct computation, we have

$$A(u^+) = u^+, \quad A(u^-) = u^-, \quad \bar{A}(u^+, u^-) = \frac{u^+ + u^-}{2}, \quad l(u^+, u^-) = \frac{1}{u^+ - u^-}.$$

Then the equation (3.2) for ξ reads

$$\xi' = D\lambda(u^+, u^-)(w^+, w^-) = \lim_{\epsilon \rightarrow 0} \frac{(u^+ + \epsilon w^+) + (u^- + \epsilon w^-)}{2\epsilon} = \frac{w_- + w_+}{2}.$$

Now we check that the new expression (3.5) gives the same relation. Indeed, we compute from (3.5) that

$$\xi' = \frac{1}{u^+ - u^-} \left(u^+ w_+ - \frac{u^+ + u^-}{2} w_+ + \frac{u^+ + u^-}{2} w_- - u^- w_- \right) = \frac{w_- + w_+}{2}.$$

In the scalar case, the last condition (3.3) does not exist. We consider the following example for the computation of both (3.2) and (3.3).

Example 2: In order to illustrate the main issues for the system case, we consider a simple 2×2 hyperbolic system

$$(3.8) \quad \begin{aligned} \partial_t \rho + \partial_x q &= 0, \\ \partial_t q + \partial_x p(\rho) &= 0, \end{aligned}$$

where $p(\rho) = \kappa \rho^\gamma$. Consider the Riemann problem

$$(\rho, q)(x, 0) = \begin{cases} (\rho^-, q^-), & x < 0, \\ (\rho^+, q^+), & x \geq 0 \end{cases}$$

with $u^- = (\rho^-, q^-)$ and $u^+ = (\rho^+, q^+)$ two constant states. We compute coefficient matrices

$$A(u^-) = \begin{pmatrix} 0 & 1 \\ p'(\rho^-) & 0 \end{pmatrix}, \quad A(u^+) = \begin{pmatrix} 0 & 1 \\ p'(\rho^+) & 0 \end{pmatrix}, \quad \bar{A}(u^+, u^-) = \begin{pmatrix} 0 & 1 \\ \bar{p}'(\rho^+, \rho^-) & 0 \end{pmatrix}$$

with $\bar{p}'(\rho^+, \rho^-) = (p(\rho^+) - p(\rho^-))/(\rho^+ - \rho^-)$ and eigenvalues

$$(3.9) \quad \lambda_1(u^+, u^-) = -\sqrt{\bar{p}'(\rho^+, \rho^-)}, \quad \lambda_2(u^+, u^-) = \sqrt{\bar{p}'(\rho^+, \rho^-)}.$$

The 1-shock is characterized by

$$(3.10) \quad q^+ - q^- = -\sqrt{(p(\rho^+) - p(\rho^-))(\rho^+ - \rho^-)}, \quad \rho^+ > \rho^-,$$

while the 2-shock is characterized by

$$(3.11) \quad q^+ - q^- = -\sqrt{(p(\rho^+) - p(\rho^-))(\rho^+ - \rho^-)}, \quad \rho^+ < \rho^-.$$

For simplicity, we show the case where only the 1-shock occurs. Namely, (ρ_+, q_+) and (ρ_-, q_-) are given by (3.10).

Next, we derive the interface conditions (3.2)-(3.3) and compare them to the new expression (3.5)-(3.6). Firstly, we denote $w^+ = (w_\rho^+, w_q^+)$ and $w^- = (w_\rho^-, w_q^-)$. A direct computation of (3.2) shows that

$$(3.12) \quad \begin{aligned} \xi' &= \lim_{\epsilon \rightarrow 0} \frac{1}{\epsilon} \left(\lambda_1(u^+ + \epsilon w_\alpha^+, u^- + \epsilon w_\alpha^-) - \lambda_1(u^+, u^-) \right) \\ &= - \left(\frac{\partial \sqrt{\bar{p}'(\rho^+, \rho^-)}}{\partial \rho^+} w_\rho^+ + \frac{\partial \sqrt{\bar{p}'(\rho^+, \rho^-)}}{\partial \rho^-} w_\rho^- \right) \\ &= - \frac{1}{2} \frac{[p'(\rho^+) - \bar{p}'(\rho^+, \rho^-)]w_\rho^+ + [\bar{p}'(\rho^+, \rho^-) - p'(\rho^-)]w_\rho^-}{(\rho^+ - \rho^-)\sqrt{\bar{p}'(\rho^+, \rho^-)}}. \end{aligned}$$

For the interface condition (3.3), we compute $l_2(u^+, u^-) = (\sqrt{\bar{p}'(\rho^+, \rho^-)}, 1)$ and thereby

$$\begin{aligned} Dl_2(u^+, u^-)(w^+, w^-) &= \lim_{\epsilon \rightarrow 0} \frac{1}{\epsilon} \left(\sqrt{\bar{p}'(\rho^+ + \epsilon w_\rho^+, \rho^- + \epsilon w_\rho^-)} - \sqrt{\bar{p}'(\rho^+, \rho^-)}, 0 \right) \\ &= \left(\frac{\partial \sqrt{\bar{p}'(\rho^+, \rho^-)}}{\partial \rho^+} w_\rho^+ + \frac{\partial \sqrt{\bar{p}'(\rho^+, \rho^-)}}{\partial \rho^-} w_\rho^-, 0 \right) \\ &= \left(\frac{1}{2} \frac{[p'(\rho^+) - \bar{p}'(\rho^+, \rho^-)]w_\rho^+ + [\bar{p}'(\rho^+, \rho^-) - p'(\rho^-)]w_\rho^-}{(\rho^+ - \rho^-)\sqrt{\bar{p}'(\rho^+, \rho^-)}}, 0 \right). \end{aligned}$$

Then the interface condition (3.3) reads as

$$\begin{aligned} 0 &= \langle l_2(u^+, u^-), w^+ - w^- \rangle + \langle Dl_2(u^+, u^-)(w^+, w^-), u^+ - u^- \rangle \\ &= \sqrt{\bar{p}'(\rho^+, \rho^-)}(w_\rho^+ - w_\rho^-) + (w_q^+ - w_q^-) \\ &\quad + \frac{1}{2} \frac{[p'(\rho^+) - \bar{p}'(\rho^+, \rho^-)]w_\rho^+ + [\bar{p}'(\rho^+, \rho^-) - p'(\rho^-)]w_\rho^-}{\sqrt{\bar{p}'(\rho^+, \rho^-)}} \\ (3.13) \quad &= (w_q^+ - w_q^-) + \frac{1}{2} \frac{p'(\rho^+)w_\rho^+ - p'(\rho^-)w_\rho^-}{\sqrt{\bar{p}'(\rho^+, \rho^-)}} + \frac{1}{2} \sqrt{\bar{p}'(\rho^+, \rho^-)}(w_\rho^+ - w_\rho^-). \end{aligned}$$

On the other hand, we use the expression in Theorem 3.1. The left eigenvector $l_1 = l_1(u^+, u^-)$ satisfying $\langle l_1, u^+ - u^- \rangle = 1$ is given by

$$l_1(u^+, u^-) = \frac{1}{2(\rho^+ - \rho^-)\sqrt{\bar{p}'(\rho^+, \rho^-)}} \left(-\sqrt{\bar{p}'(\rho^+, \rho^-)}, 1 \right).$$

Thus it follows from (3.5) that

$$\begin{aligned} \xi' &= \langle l_1(u^+, u^-), [A(u^+) - \bar{A}(u^+, u^-)]w^+ + [\bar{A}(u^+, u^-) - A(u^-)]w^- \rangle \\ &= -\frac{1}{2} \frac{[p'(\rho^+) - \bar{p}'(\rho^+, \rho^-)]w_\rho^+ + [\bar{p}'(\rho^+, \rho^-) - p'(\rho^-)]w_\rho^-}{(\rho^+ - \rho^-)\sqrt{\bar{p}'(\rho^+, \rho^-)}}, \end{aligned}$$

which is just the formula (3.12). At last, (3.6) implies

$$-\sqrt{\bar{p}'(\rho^+, \rho^-)} \begin{pmatrix} w_\rho^+ - w_\rho^- \\ w_q^+ - w_q^- \end{pmatrix} = \begin{pmatrix} w_q^+ - w_q^- \\ p'(\rho^+)w_\rho^+ - p'(\rho^-)w_\rho^- \end{pmatrix} + \xi' \begin{pmatrix} \rho^+ - \rho^- \\ q^+ - q^- \end{pmatrix}.$$

Eliminating ξ' from this equation and using (3.10) yield (3.13).

4. Numerical method. In the previous section, an explicit expression for the interface conditions at $x = x_\alpha(t)$ has been introduced. We will show that this expression can be used to design the numerical method.

4.1. Single shock case (N=1). At first, we illustrate the basic idea through a simple case where $N = 1$. Namely, there is only one discontinuous point for the solution u to the original equation (1.1). For simplicity, we drop the subscription α for ξ_α and w_α . In the equation (3.4), the interface is fixed at $y = 0$. Now we use the original spatial variable x and rewrite (3.4) as:

$$(4.1) \quad \partial_t w + \partial_x [A(u)w - \xi' u] = 0, \quad x \in (-\infty, x_\alpha) \cup (x_\alpha, +\infty).$$

Denoting $F = A(u)w - \xi'u$, we know that the weak solution satisfies

$$\int_D \left(\phi_t^T w + \phi_x^T F \right) dx dt = 0, \quad \forall \phi \in C_0^\infty(D)$$

with the domain $D \in \{x \in \mathbb{R}, t > 0\}$. Consider $D^- = \{(x, t) \in D, x < x_\alpha(t)\}$ and $D^+ = \{(x, t) \in D, x > x_\alpha(t)\}$. We compute

$$\begin{aligned} 0 &= \int_{D^-} (\phi^T w)_t + (\phi^T F)_x dx dt + \int_{D^+} (\phi^T w)_t + (\phi^T F)_x dx dt \\ &= \int_{\partial D^-} (-\phi^T w) dx + (\phi^T F) dt + \int_{\partial D^+} (-\phi^T w) dx + (\phi^T F) dt \\ &= \int_{x=x_\alpha(t)} -\phi^T (w^- - w^+) dx + \phi^T (F^- - F^+) dt \end{aligned}$$

with $F^+ = A(u^+)w^+ - \xi'u^+$ and $F^- = A(u^-)w^- - \xi'u^-$. Since ϕ is arbitrary and $dx/dt = x'_\alpha$, we conclude that

$$x'(w^+ - w^-) = A(u^+)w^+ - \xi'u^+ - A(u^-)w^- + \xi'u^-,$$

which is just (3.6).

According to the classical theory of numerical schemes for conservation laws [23], the relation (3.6) can be preserved along the discontinuity $x = x_\alpha(t)$ if we use a conservative numerical scheme to solve equation (4.1) in the domain D . Moreover, Theorem 3.1 implies that the interface condition (3.3) is satisfied. Motivated by this argument, a numerical treatment is straightforward.

Before we discuss our algorithm, we introduce some preparations. Consider a mesh on \mathbb{R} consisting of cells $I_i = (x_{i-\frac{1}{2}}, x_{i+\frac{1}{2}})$ for $i \in \mathbb{Z}$ where $x_{i+\frac{1}{2}} = (i + \frac{1}{2})\Delta x$. Here, $\Delta x > 0$ is a fixed mesh width. Moreover, we define the discrete time points $t_n = n\Delta t$ for $n \in \mathbb{Z}^+$. As in any finite volume framework, we consider the cell averages of the solution u given by $u_j^n \approx \frac{1}{\Delta x} \int_{I_j} u(t_n, x) dx$ at each $j \in \mathbb{Z}$. We assume Δt and Δx fulfill the CFL condition $\Delta t / \Delta x \max_j |\sigma(A(u_j^n))| \leq C_{CFL}$ with σ being the spectral radius. Moreover, we assume that x_α^n is a numerical approximation to the α -th jump position $x_\alpha(t_n)$. That position is obtained by using, e.g., shock capturing method or evaluation of the Rankine–Hugoniot condition, see e.g., [17]. In the present work, we compute the jump position by discretizing the Rankine–Hugoniot condition.

Having this, we propose a simple way to compute the limits u_α^- and u_α^+ at the discontinuity: (1) Choose the index J_α such that the jump position fulfills $x_\alpha^n \in I_{J_\alpha}$. (2) To reduce the effect of the numerical viscosity, we choose K according to the mesh size. Then, we consider the interval $[x_\alpha^n - K\Delta x, x_\alpha^n + K\Delta x]$. The values u_α^\pm are then defined by $u_\alpha^- = u_{J_\alpha - K}^n$ and $u_\alpha^+ = u_{J_\alpha + K}^n$, respectively. We refer to [17] for further details. The estimate of the width of the numerical viscosity layer K is non-trivial and we are not aware of a theoretical result in this direction. In this work, we therefore compute the analytical solution u and then select the parameter K to match with the analytical solution.

Some remarks are in order.

Remark 4.1. We compute the tangent vector by exploiting a conservative numerical scheme for the equation (4.1). In this way, the interface condition (3.3) is preserved automatically and no explicit discretization for this condition is needed.

For simplicity, we only present the algorithm with a first-order explicit Euler time discretization and simple numerical flux $\widehat{F}_{j+\frac{1}{2}}$. It may be possible to extend both.

Algorithm 4.1 Computation of the GTV (single-shock case)

Given data:

(1) Initial data for (1.1): the cell average $u_j^0 = \frac{1}{\Delta x} \int_{I_j} u(0, x) dx$ for $j \in \mathbb{Z}$.

(2) Initial data for the GTV: the initial shift $\xi^0 = \xi(0)$ and the cell average $v_j^0 = \frac{1}{\Delta x} \int_{I_j} v(0, x) dx$ for $j \in \mathbb{Z}$.

From u_j^0 , we reconstruct the derivatives $[u_x]_j^0$ and compute: $w_j^0 = v_j^0 + \xi^0 [u_x]_j^0$.

Updating in time from t_n to t_{n+1} :

Step 1: Update u_j^{n+1} by the conservative numerical scheme:

$$u_j^{n+1} - u_j^n + \frac{\Delta t}{\Delta x} (F_{j+\frac{1}{2}}^n - F_{j-\frac{1}{2}}^n) = 0.$$

Here $F_{j+\frac{1}{2}}^n = F(u_j^n, u_{j+1}^n)$ and F is the numerical flux function for (1.1).

Step 2: Track the shock position $x_\alpha(t_n)$ and compute the limits (u^-, u^+) and (w^-, w^+) accordingly. Then compute ξ' from (3.5) and update $\xi^{n+1} = \xi^n + \Delta t \xi'$.

Step 3: Update w_j^{n+1} by exploiting a conservative numerical scheme:

$$w_j^{n+1} - w_j^n + \frac{\Delta t}{\Delta x} (\widehat{F}_{j+\frac{1}{2}}^n - \widehat{F}_{j-\frac{1}{2}}^n) = 0.$$

Here $\widehat{F}_{j+\frac{1}{2}}^n = \widehat{F}(w_j^n, w_{j+1}^n, u_j^n, u_{j+1}^n, \xi')$ and \widehat{F} is the numerical flux function for (4.1).

Output:

We obtain u_j^n , w_j^n and ξ^n for each j and n . At last, we reconstruct the derivatives $[u_x]_j^n$ and compute the variation $v_j^n = w_j^n - \xi^n [u_x]_j^n$.

Note that our main motivation is the computation of the tangent vector. Thus, we assume that the numerical solution for the original problem (1.1) can be computed sufficiently accurate using e.g. a finer mesh than for v_j^n .

Remark 4.2. We would like to compare our method with the one developed in [8, 11] based on the delta-type source. For the case where $\partial_x u = 0$ a.e., we know that $v = w$ a.e. Then the equation (4.1) has the same form as the sensitivity equation with delta-type source term located at the discontinuity in [8, 11]. Indeed, the term $\xi' u_x$ in (4.1) corresponds to a delta function. In this particular situation, the main difference lies in the numerical treatments of the source term, e.g., we directly utilize the property of conservative schemes and do not employ shock indicators in our method. For the case where $\partial_x u$ is not necessarily zero, unlike the method in [8, 11], our strategy can be directly applied for any conservative schemes without further restriction. The last but not the least, our method also explicitly computes the jump position $x_\alpha(t)$ and its shift ξ_α by discretizing the RH condition and (3.5), which are useful in the construction of the first-order variation (2.5).

4.2. The case of multiple discontinuities . In the previous subsection, we propose a method to compute the generalized tangent vector for the case where only one jump occurs. In general, the solution u has N jumps at points $x_1(t) < x_2(t) < \dots < x_N(t)$. We use $x = y + x_\alpha(t)$ and rewrite (3.4) as:

$$(4.2) \quad \partial_t w_\alpha + \partial_x [A(u)w_\alpha - \xi'_\alpha u] = 0, \quad x \in D_\alpha.$$

Here $D_\alpha \in \mathbb{R}$ is a neighborhood of $x_\alpha(t)$ which contains no point of discontinuity of u other than $x_\alpha(t)$.

We assume there is no interaction between different jumps. Thus one can choose D_α for $\alpha = 1, 2, \dots, N$ such that $\mathbb{R} = \cup_\alpha D_\alpha$. By directly using Algorithm 4.1, we compute (4.2) to get w_α in each D_α . Next, we provide a simple method to glue all w_α together.

In each time step t_n , we take $D_\alpha^n = \{j \in \mathbb{Z} \mid j_\alpha^- \leq j \leq j_\alpha^+\}$ for each $\alpha = 1, 2, \dots, N$. The indexes $j_\alpha^-, j_\alpha^+ \in \mathbb{Z}$ and $j_{\alpha+1}^-, j_{\alpha+1}^+ \in \mathbb{Z}$ are chosen such that

$$x_{j_\alpha^- - \frac{1}{2}} \leq x_\alpha(t_n) < x_{j_\alpha^+ + \frac{1}{2}}, \quad x_{j_{\alpha+1}^- - \frac{1}{2}} \leq x_{\alpha+1}(t_n) < x_{j_{\alpha+1}^+ + \frac{1}{2}}, \quad j_\alpha^+ - J = j_{\alpha+1}^- + J.$$

where J is a nonnegative integer. It is reasonable to choose such D_α^n at each time step t^n , since no interaction of shocks occurs (by assumption). For the spatial grids $x_j \in D_\alpha^n$, we compute $w_{\alpha,j}^{n+1}$ by Algorithm 4.1. Notice that, at the point $j = j_\alpha^+$, the computation of the numerical flux depends on $w_{\alpha,j+1}^n$. Since $j+1 \in D_{\alpha+1}^n$, we only have the value of $w_{\alpha+1,j+1}^n$. Motivated by the relation (3.1), we take

$$(4.3) \quad w_{\alpha,j+1}^n = w_{\alpha+1,j+1}^n + (\xi_\alpha^n - \xi_{\alpha+1}^n)[u_x]_{j+1}^n$$

at the point $j = j_\alpha^+$.

After the computation of w_α^n for $\alpha = 1, 2, \dots, N$, we take

$$v_j^n = \begin{cases} w_{\alpha,j}^n + \xi_\alpha^n [u_x]_j^n & j_\alpha^- + J \leq j < j_\alpha^+ - J \\ w_{\alpha+1,j}^n + \xi_{\alpha+1}^n [u_x]_j^n & j_{\alpha+1}^- + J \leq j < j_{\alpha+1}^+ - J. \end{cases}$$

We end this section by presenting the numerical construction of the first-order variation. Due to the numerical viscosity, the numerical solution of u will not exhibit a jump discontinuity. Thus, a direct computation of (2.5) will lead to a spike near the jump point $x = x_\alpha(t_n)$. To avoid this phenomenon, we reconstruct the solution u by the following procedure:

1. Take the index J_α , such that the jump position $x_\alpha^n \in I_{J_\alpha}$ and take the limits u_α^-, u_α^+ by the method given in Subsection 4.1.
2. Reconstruct the solution \tilde{u}_j^n by

$$(4.4) \quad \tilde{u}_j^n = u_j^n + \sum_\alpha (u_\alpha^- - u_j^n) \chi_{[x_\alpha^n - K\Delta x, x_\alpha^n]} + \sum_\alpha (u_\alpha^+ - u_j^n) \chi_{[x_\alpha^n, x_\alpha^n + K\Delta x]}.$$

Here, $x \rightarrow \chi_{[a,b]}(x)$ is the characteristic function on the interval $[a, b]$.

Furthermore, we compute the first-order variation by

$$(4.5) \quad [u_\epsilon]_j^n = \tilde{u}_j^n + \epsilon v_j^n + \sum_{\xi_\alpha^n < 0} (u_\alpha^+ - u_\alpha^-) \chi_{[x_\alpha^n + \epsilon \xi_\alpha^n, x_\alpha^n]} - \sum_{\xi_\alpha^n > 0} (u_\alpha^+ - u_\alpha^-) \chi_{[x_\alpha^n, x_\alpha^n + \epsilon \xi_\alpha^n]}.$$

5. Numerical experiments. In this section, we present numerical experiments to show the validity of the proposed algorithm. The scalar case and the systems case are considered for the example of Burgers' equation and the 2×2 system (3.8), respectively.

In Algorithm 4.1 we use the first-order (global) Lax-Friedrichs fluxes

$$F(u_j^n, u_{j+1}^n) = \frac{1}{2} \left(f(u_j^n) + f(u_{j+1}^n) - L(u_{j+1}^n - u_j^n) \right)$$

$$\widehat{F}(w_j^n, w_{j+1}^n, u_j^n, u_{j+1}^n, \xi') = \frac{1}{2} \left(A(u_j^n) w_j^n - \xi' u_j^n + A(u_{j+1}^n) w_{j+1}^n - \xi' u_{j+1}^n - L(w_{j+1}^n - w_j^n) \right).$$

Here, $L = \max_j |\sigma(A(u_j^n))|$ and σ is the spectral radius.

5.1. Scalar case: Burgers' equation. For Burger's equation

$$u_t + \left(\frac{u^2}{2}\right)_x = 0,$$

we consider the example in [5] where the initial data is given by

$$u(0, x) = (1 + \epsilon)x \cdot \chi_{[0,1]}(x).$$

The exact solution is

$$(5.1) \quad u^\epsilon(t, x) = \frac{(1 + \epsilon)x}{1 + (1 + \epsilon)t} \cdot \chi_{[0, \sqrt{1+(1+\epsilon)t}]}(x).$$

As derived in Section 4, the equations for (w, ξ) read

$$w_t + (uw - \xi u)_x = 0, \quad \xi' = \frac{w_- + w_+}{2}.$$

Here are some details about the computation. We choose the time step Δt to satisfy the CFL condition with $C_{CFL} = 0.1$. We partition the spatial interval $[0, 2]$ into N_x cells with $N_x = 20000$. Moreover, in the implementation of Algorithm 4.1, we take the limits (w^-, w^+) , (u^-, u^+) as discussed in Section 4.1 with a viscosity parameter of $K = 10$. We obtain the jump position x_α^n by computing the Rankine–Hugoniot condition

$$x_\alpha^{n+1} = x_\alpha^n + \frac{\Delta t}{2}(u^+ + u^-).$$

We compute the results up to time $t = 0.2$. We obtain the numerical results $x_\alpha(t)|_{t=0.2} = 1.0953$ for the jump position and $\xi(t)|_{t=0.2} = 0.0914$ for the generalized tangent vector. To compare it with the theoretical result, we also compute x_α and ξ from the exact solution [5]:

$$x_\alpha^{exact} = \sqrt{1+t} = 1.0954, \quad \xi^{exact} = \frac{t}{2\sqrt{1+t}} = 0.0913.$$

From this computation, we see that the numerical solution for ξ is very close to the exact value with a relative error $e_\xi = |\xi - \xi^{exact}|/\xi^{exact} \approx 0.1\%$.

Having the numerical results for u , w , x_α , u^\pm , and ξ at $t = 0.2$, we construct the first-order variation u_ϵ by

$$u_\epsilon(x, t) = u(x, t) + \epsilon[w(x, t) - \xi u_x(x, t)] - [u^+ - u^-]\chi_{[x_\alpha, x_\alpha + \epsilon\xi]}(x).$$

The function u is reconstructed according to (4.4). For the derivative u_x , we first compute u_x^f and u_x^b by $[u_x^f]_j^n = (u_{j+1}^n - u_j^n)/\Delta x$ and $[u_x^b]_j^n = (u_j^n - u_{j-1}^n)/\Delta x$. Then we construct u_x by

$$u_x = \begin{cases} u_x^f & |u_x^f| < |u_x^b|, \\ u_x^b & |u_x^f| \geq |u_x^b|. \end{cases}$$

We plot the first-order variation and the exact solution with $\epsilon = 0.05$ in Fig. 1 (left). This experiment also validates that our method works for the case where $\partial_x u \neq 0$. The theoretical result in [5] indicates that the L^1 -norm $\|(u^\epsilon - u_\epsilon)/\epsilon\|_{L^1}$ should converge to 0 as $\epsilon \rightarrow 0$. To verify this, we compute $\|u^\epsilon - u_\epsilon\|_{L^1}$ for $\epsilon = 0.05 \times 1.5^i$ with $0 \leq i \leq 5$ and plot the convergence result in Fig 1 (right). In this example, we use the analytical solutions for u^ϵ in (5.1). The dashed line represents the exact second-order convergence rate. From this figure, we see that the difference $\|u^\epsilon - u_\epsilon\|_{L^1}$ is of order ϵ^2 . This implies that u_ϵ is a valid first-order approximation for u^ϵ in the sense of L^1 norm.

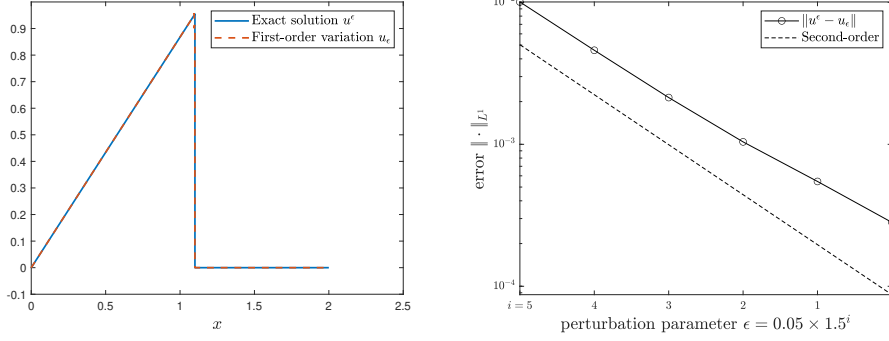


FIG. 1. *Burger's equation: (left) the exact solution u^ϵ and the first-order variation u_ϵ computed from the GTV at $t = 0.2$; (right) the difference $\|u^\epsilon - u_\epsilon\|_{L^1}$ between the exact solution and the first-order variation with different ϵ .*

5.2. The 2×2 system with single shock. We consider the 2×2 hyperbolic system in Section 3:

$$(5.2) \quad \begin{cases} \partial_t \rho + \partial_x q = 0, \\ \partial_t q + \partial_x p(\rho) = 0, \end{cases}$$

where $p(\rho) = \kappa \rho^\gamma$. In what follows, we set $\kappa = 1$ and $\gamma = 2$. Consider the Riemann problem

$$(\rho^\epsilon, q^\epsilon)(0, x) = \begin{cases} (2 + 2\epsilon, 0), & x < 0, \\ (1 + \epsilon, -\sqrt{3}(1 + \epsilon)^{3/2}), & x \geq 0. \end{cases}$$

A simple computation shows that the initial data is given on the curve (3.10). Therefore, for any ϵ , only the 2-shock occurs and the exact solution is

$$(5.3) \quad (\rho^\epsilon, q^\epsilon)(t, x) = \begin{cases} (2 + 2\epsilon, 0), & x < \sqrt{3(1 + \epsilon)} t, \\ (1 + \epsilon, -\sqrt{3}(1 + \epsilon)^{3/2}), & x \geq \sqrt{3(1 + \epsilon)} t. \end{cases}$$

At first, we compute the initial data for (ξ, w) . By the Taylor's expansion, we have $-\sqrt{3}(1 + \epsilon)^{3/2} = -\sqrt{3} - \frac{3\sqrt{3}}{2}\epsilon + O(\epsilon^2)$. Then the initial data is

$$\xi(0) = 0, \quad w(x, 0) = \begin{cases} (2, 0), & x < 0, \\ (1, -\frac{3\sqrt{3}}{2}), & x \geq 0. \end{cases}$$

Now we use Algorithm 4.1 to compute the generalized tangent vector (ξ, v) . We take the CFL number as $C_{CFL} = 0.5$ and partition the spatial interval $[-\pi, \pi]$ into N_x cells with $N_x = 20'000$. At the boundary, the numerical flux is set to zero. Moreover, the jump position x_α^n is determined by solving the Rankine–Hugoniot condition

$$x_\alpha^{n+1} = x_\alpha^n + \Delta t \frac{q^+ - q^-}{\rho^+ - \rho^-}.$$

Here the limits (ρ^\pm, q^\pm) and (w_ρ^\pm, w_q^\pm) are evaluated following the procedure outlined in Section 4.1. In this context, the viscosity parameter is set to $K = 20$.

We compute the results at $t = 0.5$. Namely, $x_\alpha|_{t=0.5} = 0.8663$, $\xi|_{t=0.5} = 0.4328$ and $w|_{t=0.5} = (w_\rho, w_q)|_{t=0.5}$ is shown in Fig. 2 (left). From the exact solution (5.3), we compute the theoretical results:

$$x_\alpha^{exact}|_{t=0.5} = 0.8660, \quad \xi^{exact}|_{t=0.5} = \lim_{\epsilon \rightarrow 0} \frac{\sqrt{3(1+\epsilon)t} - \sqrt{3t}}{\epsilon} \Big|_{t=0.5} = 0.4330.$$

Thus we see that the numerical solution for ξ is very close to the theoretical result with a relative error $e_\xi = |\xi - \xi^{exact}|/\xi^{exact} \approx 0.05\%$.

To show the importance of the interface condition (2.4), we also plot the numerical result by directly computing (2.2) in Fig. 2 (right). Namely, we use the first-order Lax-Friedrichs scheme to compute (2.2) without considering the interface condition (2.4). At $t = 0.05$, we observe the incorrect spike near the shock position. This test shows the necessity to prescribe the correct interface condition.

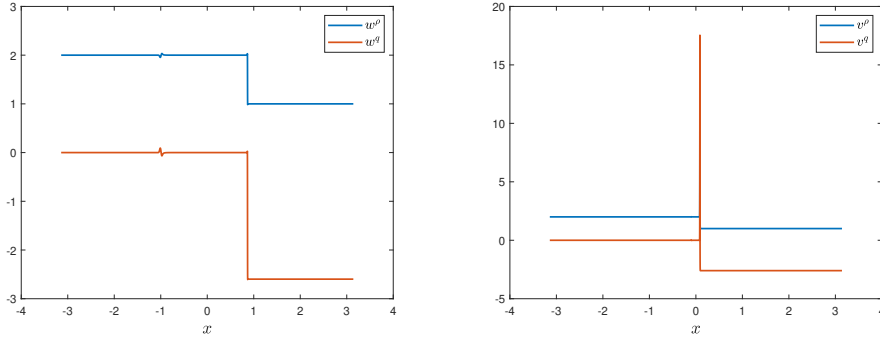


FIG. 2. Single shock case for the system (5.2): (left) the numerical solution of $w = (w_\rho, w_q)$ at $t = 0.5$ by using Algorithm 4.1. (right) the numerical solution of $v = (v_\rho, v_q)$ at $t = 0.05$ by directly computing (2.2). This test shows the necessity to prescribe the correct interface condition.

To verify that the computed generalized tangent vector is correct, we construct the first-order variation by

$$(5.4) \quad \begin{pmatrix} \rho_\epsilon \\ q_\epsilon \end{pmatrix} = \begin{pmatrix} \rho \\ q \end{pmatrix} + \epsilon \begin{pmatrix} w_\rho \\ w_q \end{pmatrix} - \begin{pmatrix} \rho^+ - \rho^- \\ q^+ - q^- \end{pmatrix} \chi_{[x_\alpha, x_\alpha + \epsilon \xi]}.$$

Here (ρ, q) , (w_ρ, w_q) , (ρ^\pm, q^\pm) , x_α and ξ are given by the numerical results at $t = 0.5$. We use the reconstruction of (ρ, q) by (4.4). Having this first-order variation, we compare it with the exact solution $(\rho^\epsilon, q^\epsilon)(t, x)$ at $t = 0.5$. For $\epsilon = 0.05$, we plot in Fig. 3 the first-order variation $(\rho_\epsilon, q_\epsilon)$ by (5.4) and the exact solution by (5.3). Furthermore, we compute the L^1 -norm of the difference $(\rho^\epsilon - \rho_\epsilon, q^\epsilon - q_\epsilon)$. Theoretically, we know that $\|(\rho^\epsilon - \rho_\epsilon, q^\epsilon - q_\epsilon)/\epsilon\|_{L^1} \rightarrow 0$ as $\epsilon \rightarrow 0$. With different ϵ , we compute the convergence rate in Fig 4. The analytical solutions for $(\rho^\epsilon, q^\epsilon)$ are used in equation (5.3). Similar to the case of Burgers' equation, the difference $\|(\rho^\epsilon - \rho_\epsilon, q^\epsilon - q_\epsilon)\|_{L^1}$ is of order ϵ^2 . This implies that $(\rho_\epsilon, q_\epsilon)$ is a first-order approximation in L^1 .

5.3. The 2×2 system with two shocks. In this subsection, we also consider the system (5.2) with $\kappa = 1$ and $\gamma = 2$. By properly choosing the initial data, we

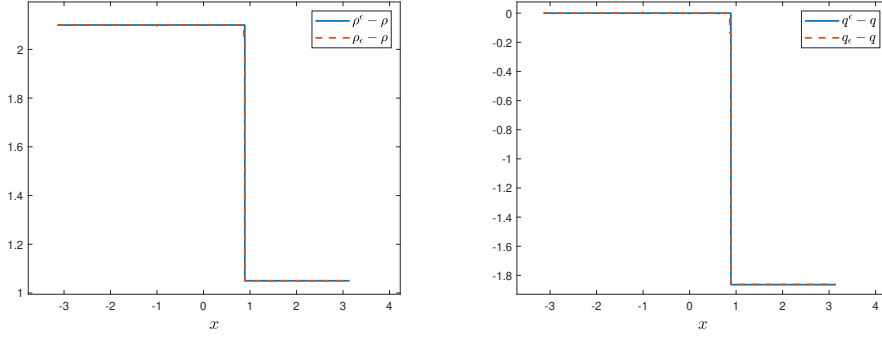


FIG. 3. Single shock case for the system (5.2): the variation $(\rho^\epsilon - \rho^0, q^\epsilon - q^0)$ by solving the original problem and $(\rho_\epsilon - \rho^0, q_\epsilon - q^0)$ by computing the generalized tangent vector.

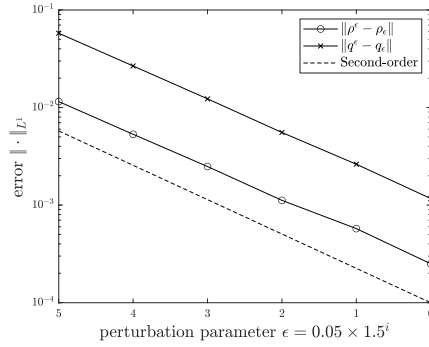


FIG. 4. Single shock case for the system (5.2): the difference $\|(\rho^\epsilon - \rho_\epsilon, q^\epsilon - q_\epsilon)\|_{L^1}$ between the exact solution and the first-order variation.

construct an example with two shocks. The initial data is given by

$$(\rho^0, q^0)(0, x) = \begin{cases} (2, 0) & x < x_1(0), \\ (2.241, -0.4963) & x_1(0) < x < x_2(0), \\ (1, -2.7304) & x > x_2(0). \end{cases}$$

Here $x_1(t) = -2.0593(t + 0.1)$ and $x_2(t) = 1.8002(t + 0.1)$. Now we consider the perturbation of the initial data

$$\begin{pmatrix} \rho^\epsilon \\ q^\epsilon \end{pmatrix}(0, x) = \begin{pmatrix} \rho^0 \\ q^0 \end{pmatrix}(0, x) + \epsilon \begin{pmatrix} w_\rho \\ w_q \end{pmatrix}(0, x), \quad x_i^\epsilon(0) = x_i(0) + \epsilon \xi_i(0), \quad i = 1, 2$$

with $\xi_1(0) = -0.0728$, $\xi_2(0) = 0.05554$ and

$$(w_\rho, w_q)(0, x) = \begin{cases} (2, -1.8839) & x < x_1(0), \\ (1, 0) & x_1(0) < x < x_2(0), \\ (1, -0.6893) & x > x_2(0). \end{cases}$$

With this initial condition, we compute the numerical solutions of $(\rho^\epsilon, q^\epsilon)$ for different ϵ by using the first-order finite volume scheme with Lax–Friedrichs flux. The spatial

interval $[-\pi, \pi]$ is divided into N_x cells with $N_x = 20'000$. On the other hand, we compute w_ρ and w_q by using Algorithm 4.1 and the strategy in Section 4.2. In this case, the value of u_x in (4.3) is equivalent to zero. This computation uses CFL number $C_{CFL} = 0.1$. The spatial interval $[-\pi, \pi]$ is also divided into N_x cells with $N_x = 20'000$. At the boundary, we take the numerical flux to be zero. We take the limits (ρ^\pm, q^\pm) and (w_ρ^\pm, w_q^\pm) at each time step by exploiting the method in Section 4.1 with the viscosity parameter $K = 50$. Having (w_ρ, w_q) , we compute the first-order variation according to the formula (4.5). Note that we also use the reconstruction of u by (4.4).

In Fig 5, we compare the computed first-order variation $(\rho_\epsilon, q_\epsilon)$ to the solution $(\rho^\epsilon, q^\epsilon)$ of the original system (5.2) with parameter $\epsilon = 0.05$. Out of this figure, we observe that the first-order variation approximates the original solution well. There are small oscillations visible near the shock positions, see Fig. 6 for zoomed-in details. In fact, this phenomenon also occurs for the theoretical result. More precisely, in the construction (2.5), the jump position for u is shifted to $x_\alpha + \epsilon\xi_\alpha$ while the jump position for v stays in x_α .

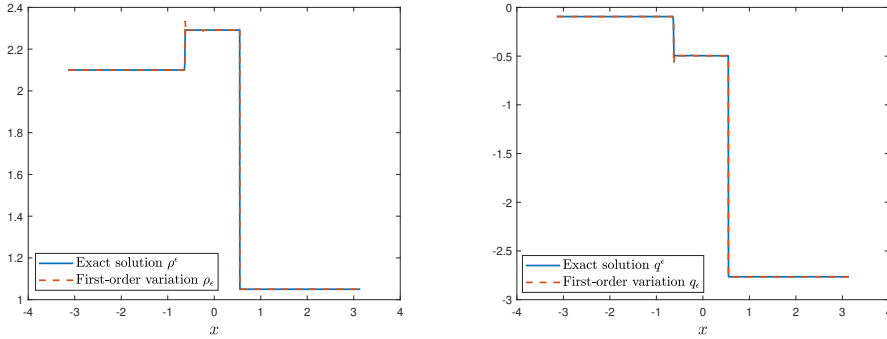


FIG. 5. Two shocks case for the system (5.2): The solution $(\rho^\epsilon, q^\epsilon)$ to the system (5.2) and the first-order variation $(\rho_\epsilon, q_\epsilon)$ computed from the GTV at $t = 0.2$.

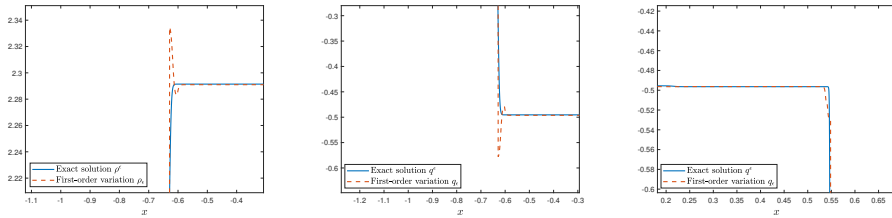


FIG. 6. Two shocks case for the system (5.2): The solution $(\rho^\epsilon, q^\epsilon)$ to the system (5.2) and the first-order variation $(\rho_\epsilon, q_\epsilon)$ computed from the GTV at $t = 0.2$. Details near $x = x_1(t)$ are shown in the first two figures and the detail near $x = x_2(t)$ is shown in the last figure.

For the perturbation of the jump position, the numerical result gives

$$(5.5) \quad \xi_1(t)|_{t=0.2} = -0.2184, \quad \xi_2(t)|_{t=0.2} = 0.1666.$$

For this example, obtaining the exact results for ξ_1 and ξ_2 is not trivial. However, due to the choice of the initial data, $(\rho^\epsilon, q^\epsilon)|_{t=0}$ are approximately given on the shock

curves (3.10) and (3.11) with an error $O(\epsilon^2)$. Thus, we have the following approximate solution for sufficiently small ϵ

$$(\rho^\epsilon, q^\epsilon)(0, x) \approx \begin{cases} (2 + 2\epsilon, -1.8839\epsilon) & x < x_1^\epsilon(t), \\ (2.241 + \epsilon, -0.4963) & x_1^\epsilon(t) < x < x_2^\epsilon(t), \\ (1 + \epsilon, -2.7304 - 0.6893\epsilon) & x > x_2^\epsilon(t), \end{cases}$$

where

$$x_1^\epsilon(t) = \frac{-0.4963 + 1.8839\epsilon}{0.241 - \epsilon}(t + 0.1) = (-2.0593 - 0.728\epsilon)(t + 0.1) + O(\epsilon^2),$$

$$x_2^\epsilon(t) = \frac{-2.2341 - 0.6893\epsilon}{-1.241}(t + 0.1) = (1.8002 + 0.5554\epsilon)(t + 0.1) + O(\epsilon^2).$$

For comparison, we compute

$$\left. \frac{x_1^\epsilon(t) - x_1(t)}{\epsilon} \right|_{t=0.2} = -0.2184 + O(\epsilon), \quad \left. \frac{x_2^\epsilon(t) - x_2(t)}{\epsilon} \right|_{t=0.2} = 0.1666 + O(\epsilon).$$

This matches the numerical result in (5.5).

In order to validate the numerical approximation to the tangent vector (w_ρ, w_q) and (ξ_1, ξ_2) , we compute the convergence rate of $\|(\rho^\epsilon - \rho_\epsilon, q^\epsilon - q_\epsilon)\|_{L^1}$ in Fig 7 (left) with different ϵ . Similarly to the previous cases, we see that the difference $\|(\rho^\epsilon - \rho_\epsilon, q^\epsilon - q_\epsilon)\|_{L^1}$ is approximately of order ϵ^2 for sufficiently small ϵ . This implies that $(\rho_\epsilon, q_\epsilon)$ is a first-order approximation in L^1 . We observe that the convergence rate levels out as ϵ becomes small. This is due to the numerical errors in solving the equations. When $\epsilon = 0.05$, the error $\|(\rho^\epsilon - \rho_\epsilon, q^\epsilon - q_\epsilon)\|_{L^1} = O(10^{-4})$, which is of the order of the mesh size. To verify this, we also show the convergence result by using a finer grid with $N_x = 40'000$.

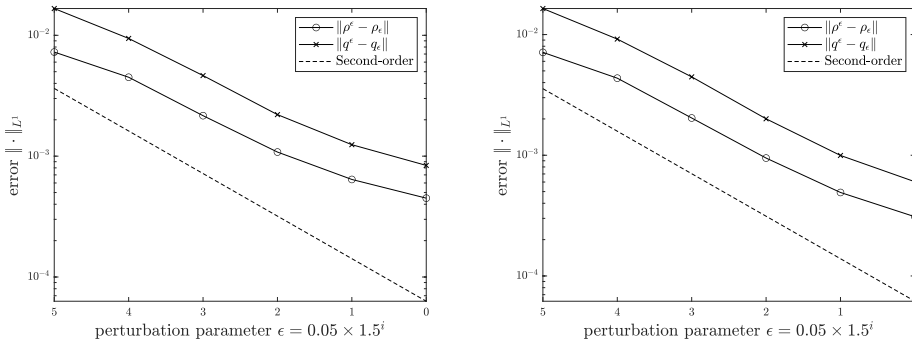


FIG. 7. Two shocks case for the system (5.2): the difference $\|(\rho^\epsilon - \rho_\epsilon, q^\epsilon - q_\epsilon)\|_{L^1}$ between the exact solution and the first-order variation at $t = 0.2$. Left: numerical solution with $N_x = 20'000$, Right: numerical solution with $N_x = 40'000$.

6. Outlook. This work discusses a possible numerical computation of the generalized tangent vector and focuses on the numerical treatment for the interface conditions across discontinuities. We develop a simple numerical method in the framework of conservative schemes, enabling the automatic preservation of interface conditions without explicit discretization. A possible future work is to combine the strategy with

other effective schemes, e.g. high-order Runge-Kutta discontinuous Galerkin scheme to reduce the numerical viscosity.

Appendix A. Details of the proof in Section 3.

We give the proof of Lemma 3.2 by some tensor computations.

Proof. According to the definition of l_i , we have

$$(A.1) \quad l_i(u^+, u^-) \bar{A}(u^+, u^-) = \lambda_i(u^+, u^-) l_i(u^+, u^-), \quad i = 1, 2, \dots, n.$$

The derivatives $\partial/\partial u^+$ are computed on both sides. Note that $\partial \bar{A}(u^+, u^-)/\partial u^+$ is a third-order tensor. To simplify the notation, we use the Einstein summation convention and write (A.1) as

$$l_{ih} \bar{A}_{hj} = \lambda_i l_{ij}, \quad i, j = 1, 2, \dots, n.$$

Taking derivative $\partial/\partial u_m^+$ on both sides (u_m^+ is the m -th component of u^+), we obtain

$$\frac{\partial l_{ih}}{\partial u_m^+} \bar{A}_{hj} + l_{ih} \frac{\partial \bar{A}_{hj}}{\partial u_m^+} = \frac{\partial \lambda_i}{\partial u_m^+} l_{ij} + \frac{\partial l_{ij}}{\partial u_m^+} \lambda_i.$$

Multiplying the relation with $(u_j^+ - u_j^-)$ and summing j from 1 to n , we have

$$\frac{\partial l_{ih}}{\partial u_m^+} \bar{A}_{hj} (u_j^+ - u_j^-) + l_{ih} \frac{\partial \bar{A}_{hj}}{\partial u_m^+} (u_j^+ - u_j^-) = \frac{\partial \lambda_i}{\partial u_m^+} l_{ij} (u_j^+ - u_j^-) + \frac{\partial l_{ij}}{\partial u_m^+} \lambda_i (u_j^+ - u_j^-).$$

Since $\bar{A}_{hj} (u_j^+ - u_j^-) = \lambda_{k_\alpha} (u_h^+ - u_h^-)$, we have

$$(A.2) \quad \frac{\partial l_{ih}}{\partial u_m^+} (\lambda_{k_\alpha} - \lambda_i) (u_h^+ - u_h^-) + l_{ih} \frac{\partial \bar{A}_{hj}}{\partial u_m^+} (u_j^+ - u_j^-) = \frac{\partial \lambda_i}{\partial u_m^+} (l_{ij}, u_j^+ - u_j^-).$$

To simplify the second term, we compute

$$\frac{\partial \bar{A}_{hj}}{\partial u_m^+} = \int_0^1 \frac{\partial}{\partial u_m^+} [A_{hj}(\theta u^+ + (1-\theta)u^-)] d\theta = \int_0^1 \theta \frac{\partial A_{hj}}{\partial u_m} (\theta u^+ + (1-\theta)u^-) d\theta.$$

Besides, by the definition of $A(u)$, we know that

$$\frac{\partial A_{hj}}{\partial u_m} = \frac{\partial^2 F_h}{\partial u_m \partial u_j} = \frac{\partial^2 F_h}{\partial u_j \partial u_m} = \frac{\partial A_{hm}}{\partial u_j}.$$

Thus it follows that

$$\begin{aligned} \frac{\partial \bar{A}_{hj}}{\partial u_m^+} (u_j^+ - u_j^-) &= \int_0^1 \theta \frac{\partial A_{hm}}{\partial u_j} (\theta u^+ + (1-\theta)u^-) (u_j^+ - u_j^-) d\theta \\ &= \int_0^1 \theta \frac{d}{d\theta} [A_{hm}(\theta u^+ + (1-\theta)u^-)] \\ &= \theta A_{hm}(\theta u^+ + (1-\theta)u^-) \Big|_0^1 - \int_0^1 A_{hm}(\theta u^+ + (1-\theta)u^-) d\theta \\ &= A_{hm}(u^+) - \bar{A}_{hm}(u^+, u^-). \end{aligned}$$

Substituting this into (A.2), we have

$$\frac{\partial l_{ih}}{\partial u_m^+} (\lambda_{k_\alpha} - \lambda_i) (u_h^+ - u_h^-) + l_{ih} [A_{hm}(u^+) - \bar{A}_{hm}(u^+, u^-)] = \frac{\partial \lambda_i}{\partial u_m^+} (l_{ij}, u_j^+ - u_j^-).$$

This is the first relation in Lemma 3.2. For the second case, the proof is quite similar and we omit it. \square

In the next, we clarify the notation $\langle Dl_i(u^+, u^-)(w^+, w^-), u^+ - u^- \rangle$ in (3.3):

$$Dl_{ih}(u^+, u^-)(w^+, w^-) = \lim_{\epsilon \rightarrow 0} \frac{l_{ih}(u^+ + \epsilon w^+, u^- + \epsilon w^-)}{\epsilon} = \frac{\partial l_{ih}}{\partial u_m^+} w_m^+ + \frac{\partial l_{ih}}{\partial u_m^-} w_m^-.$$

Thus we have

$$\langle Dl_i(u^+, u^-)(w^+, w^-), u^+ - u^- \rangle = \frac{\partial l_{ih}}{\partial u_m^+} w_m^+ (u_h^+ - u_h^-) + \frac{\partial l_{ih}}{\partial u_m^-} w_m^- (u_h^+ - u_h^-).$$

REFERENCES

- [1] M. K. BANDA AND M. HERTY, *Adjoint IMEX-based schemes for control problems governed by hyperbolic conservation laws*, *Comput. Optim. Appl.*, 51 (2012), pp. 909–930, <https://doi.org/10.1007/s10589-010-9362-2>.
- [2] S. BIANCHINI, *On the shift differentiability of the flow generated by a hyperbolic system of conservation laws*, *Discrete Contin. Dynam. Systems*, 6 (2000), pp. 329–350, <https://doi.org/10.3934/dcds.2000.6.329>.
- [3] A. BRESSAN, *Hyperbolic systems of conservation laws*, vol. 20 of Oxford Lecture Series in Mathematics and its Applications, Oxford University Press, Oxford, 2000. The one-dimensional Cauchy problem.
- [4] A. BRESSAN AND G. GUERRA, *Shift-differentiability of the flow generated by a conservation law*, *Discrete Contin. Dynam. Systems*, 3 (1997), pp. 35–58, <https://doi.org/10.3934/dcds.1997.3.35>.
- [5] A. BRESSAN AND A. MARSON, *A variational calculus for discontinuous solutions of systems of conservation laws*, *Comm. Partial Differential Equations*, 20 (1995), pp. 1491–1552, <https://doi.org/10.1080/03605309508821142>.
- [6] A. BRESSAN AND W. SHEN, *Optimality conditions for solutions to hyperbolic balance laws*, in *Control methods in PDE-dynamical systems*, vol. 426 of *Contemp. Math.*, Amer. Math. Soc., Providence, RI, 2007, pp. 129–152, <https://doi.org/10.1090/conm/426/08187>.
- [7] C. CASTRO, F. PALACIOS, AND E. ZUAZUA, *An alternating descent method for the optimal control of the inviscid Burgers equation in the presence of shocks*, *Math. Models Methods Appl. Sci.*, 18 (2008), pp. 369–416, <https://doi.org/10.1142/S0218202508002723>.
- [8] C. CHALONS, R. DUVERGNEAU, AND C. FIORINI, *Sensitivity analysis and numerical diffusion effects for hyperbolic PDE systems with discontinuous solutions. The case of barotropic Euler equations in Lagrangian coordinates*, *SIAM J. Sci. Comput.*, 40 (2018), pp. A3955–A3981, <https://doi.org/10.1137/17M1140807>.
- [9] A. CHERTOCK, M. HERTY, AND A. KURGANOV, *An Eulerian-Lagrangian method for optimization problems governed by multidimensional nonlinear hyperbolic PDEs*, *Comput. Optim. Appl.*, 59 (2014), pp. 689–724, <https://doi.org/10.1007/s10589-014-9655-y>.
- [10] C. D’APICE, R. MANZO, AND B. PICCOLI, *Numerical schemes for the optimal input flow of a supply chain*, *SIAM J. Numer. Anal.*, 51 (2013), pp. 2634–2650, <https://doi.org/10.1137/120889721>.
- [11] C. FIORINI, C. CHALONS, AND R. DUVERGNEAU, *A modified sensitivity equation method for the Euler equations in presence of shocks*, *Numer. Methods Partial Differential Equations*, 36 (2020), pp. 839–867, <https://doi.org/10.1002/num.22454>.
- [12] M. GILES AND S. ULBRICH, *Convergence of linearized and adjoint approximations for discontinuous solutions of conservation laws. Part 1: Linearized approximations and linearized output functionals*, *SIAM J. Numer. Anal.*, 48 (2010), pp. 882–904, <https://doi.org/10.1137/080727464>.
- [13] M. GILES AND S. ULBRICH, *Convergence of linearized and adjoint approximations for discontinuous solutions of conservation laws. Part 2: Adjoint approximations and extensions*, *SIAM J. Numer. Anal.*, 48 (2010), pp. 905–921, <https://doi.org/10.1137/09078078X>.
- [14] M. B. GILES, M. C. DUTA, J.-D. MULLER, AND N. A. PIERCE, *Algorithm developments for discrete adjoint methods*, *AIAA Journal*, 41 (2003), pp. 198–205, <https://doi.org/10.2514/2.1961>.
- [15] V. GUINOT, *Upwind finite volume solution of sensitivity equations for hyperbolic systems of conservation laws with discontinuous solutions*, *Comput. & Fluids*, 38 (2009), pp. 1697–1709, <https://doi.org/10.1016/j.compfluid.2009.03.002>.
- [16] V. GUINOT, C. DELENNE, AND B. CAPPELAERE, *An approximate riemann solver for sensitivity equations with discontinuous solutions*, *Advances in Water Resources*, 32 (2009), pp. 61–77, <https://doi.org/https://doi.org/10.1016/j.advwatres.2008.10.002>.

- [17] M. HERTY, J. HÜSER, U. NAUMANN, T. SCHILDEN, AND W. SCHRÖDER, *Algorithmic differentiation of hyperbolic flow problems*, J. Comput. Phys., 430 (2021), pp. Paper No. 110110, 17, <https://doi.org/10.1016/j.jcp.2021.110110>.
- [18] M. HERTY, A. KURGANOV, AND D. KUROCHKIN, *Numerical method for optimal control problems governed by nonlinear hyperbolic systems of PDEs*, Commun. Math. Sci., 13 (2015), pp. 15–48, <https://doi.org/10.4310/CMS.2015.v13.n1.a2>.
- [19] M. HERTY, A. KURGANOV, AND D. KUROCHKIN, *On convergence of numerical methods for optimization problems governed by scalar hyperbolic conservation laws*, in Theory, numerics and applications of hyperbolic problems. I, vol. 236 of Springer Proc. Math. Stat., Springer, Cham, 2018, pp. 691–706, https://doi.org/10.1007/978-3-319-91545-6_5.
- [20] M. HERTY AND B. PICCOLI, *A numerical method for the computation of tangent vectors to 2×2 hyperbolic systems of conservation laws*, Commun. Math. Sci., 14 (2016), pp. 683–704, <https://doi.org/10.4310/CMS.2016.v14.n3.a5>.
- [21] A. JAMESON AND L. MARTINELLI, *Aerodynamic shape optimization techniques based on control theory*, in Computational mathematics driven by industrial problems (Martina Franca, 1999), vol. 1739 of Lecture Notes in Math., Springer, Berlin, 2000, pp. 151–221, <https://doi.org/10.1007/BFb0103920>.
- [22] P. D. LAX, *Hyperbolic systems of conservation laws. II*, Comm. Pure Appl. Math., 10 (1957), pp. 537–566, <https://doi.org/10.1002/cpa.3160100406>.
- [23] R. J. LEVEQUE, *Finite volume methods for hyperbolic problems*, Cambridge Texts in Applied Mathematics, Cambridge University Press, Cambridge, 2002, <https://doi.org/10.1017/CBO9780511791253>.
- [24] T. LIARD AND E. ZUAZUA, *Initial data identification for the one-dimensional burgers equation*, IEEE Transactions on Automatic Control, 67 (2022), pp. 3098–3104, <https://doi.org/10.1109/TAC.2021.3096921>.
- [25] Y. OU AND P. ZHU, *The vanishing viscosity method for the sensitivity analysis of an optimal control problem of conservation laws in the presence of shocks*, Nonlinear Anal. Real World Appl., 14 (2013), pp. 1947–1974, <https://doi.org/10.1016/j.nonrwa.2013.02.001>.
- [26] N. A. PIERCE AND M. B. GILES, *Adjoint and defect error bounding and correction for functional estimates*, J. Comput. Phys., 200 (2004), pp. 769–794, <https://doi.org/10.1016/j.jcp.2004.05.001>.
- [27] P. SCHÄFER AGUILAR, J. M. SCHMITT, S. ULBRICH, AND M. MOOS, *On the numerical discretization of optimal control problems for conservation laws*, Control Cybern., 48 (2019), pp. 345–375.
- [28] P. SCHÄFER AGUILAR AND S. ULBRICH, *Convergence of numerical adjoint schemes arising from optimal boundary control problems of hyperbolic conservation laws*, Tech. Report TRR154 Preprint No. 481, Department of Mathematics, TU Darmstadt, 2021, <https://opus4.kobv.de/opus4-trr154/files/481/SchaeferAguilarUlbrichpapernumadjoint.pdf>.
- [29] J. M. SCHMITT AND S. ULBRICH, *Optimal boundary control of hyperbolic balance laws with state constraints*, SIAM J. Control Optim., 59 (2021), pp. 1341–1369, <https://doi.org/10.1137/19M129797X>.
- [30] S. ULBRICH, *Optimal control of nonlinear hyperbolic conservation laws with source terms*, Habilitation, (2001).
- [31] S. ULBRICH, *A sensitivity and adjoint calculus for discontinuous solutions of hyperbolic conservation laws with source terms*, SIAM J. Control Optim., 41 (2002), pp. 740–797, <https://doi.org/10.1137/S0363012900370764>.
- [32] S. ULBRICH, *Adjoint-based derivative computations for the optimal control of discontinuous solutions of hyperbolic conservation laws*, vol. 48, 2003, pp. 313–328, [https://doi.org/10.1016/S0167-6911\(02\)00275-X](https://doi.org/10.1016/S0167-6911(02)00275-X). Optimization and control of distributed systems.